0013-7227/02/$15.00/0
Printed in U.S.A.

Endocrinology 143(12):4875–4885

doi: 10.1210/en.2002-220558

Expression of the *Pem* Homeobox Gene in Sertoli Cells Increases the Frequency of Adjacent Germ Cells with Deoxyribonucleic Acid Strand Breaks

CHAD M. WAYNE, KEITH SUTTON, AND MILES F. WILKINSON

Department of Immunology, The University of Texas M. D. Anderson Cancer Center, Houston, Texas 77030

Pem is a member of the homeobox transcription factor family that is expressed in somatic cells in male and female reproductive tissues. In the murine testis, Pem is specifically expressed in Sertoli cells, where it is dramatically induced at the initiation of meiosis during the first wave of spermatogenesis and then later is restricted to stages IV–VIII of the seminiferous epithelial cycle. To study the function of Pem in Sertoli cells, we generated transgenic mice that express Pem in Sertoli cells during all stages of the seminiferous epithelial cycle. This resulted in a large increase (6-fold) in the number of preleptotene spermatocytes with double-strand DNA breaks and a modest increase (2.5-fold) in the number of elongating spermatids (steps 9 and 10) with single-strand DNA breaks, based on terminal deoxynucleotidyltransferase-mediated deoxyuridine 5′-triphosphate nick end labeling and comet analysis. The average number of DNA strand breaks in these germ cell populations also increased. Despite the transient increase in DNA strand breaks, Pem transgenic mice exhibited no significant anomalies in spermatogenesis, fertility, or fecundity. Our results suggest that Pem regulates Sertoli-cell genes that encode secreted or cell-surface proteins that serve to control premeiotic DNA replication, DNA repair, and/or chromatin remodeling in the adjacent germ cells. (*Endocrinology* 143: 4875–4885, 2002)

SERTOLI CELLS ARE essential for spermatogenesis because they provide many functions required for the viability and maturation of the germ cells that they cradle. Sertoli cells provide physical support for germ cells; phagocytose residual cytoplasmic bodies and apoptotic germ cells; form the blood-testis barrier; promote germ cell meiosis by lifting spermatocytes from the basal to the adluminal compartments; play an active role in the release of spermatozoa from the seminiferous epithelium; provide nutrients for germ cells; and secrete a variety of factors hypothesized to influence germ cell function and behavior (1, 2). Though Sertoli cell-germ cell interactions are essential for an organism to produce viable mature germ cells, it is not clear whether Sertoli cells only serve a nursing function or whether they also direct germ cell maturation events (2, 3).

In this communication, we provide evidence that *Pem*, a member of the homeobox transcription factor family expressed in Sertoli cells (4–7), regulates events associated with germ cell maturation in the adult testis. Homeobox transcription factors are best known for regulating embryonic developmental events, including axis formation and the specification of segment identity (8). In contrast, little is known about their role in postnatal and adult development. For example, although many Hox homeobox transcription factors are expressed in germ cells in the adult testis, it is not clear whether they function there (9, 10). Among all known homeobox proteins expressed in the adult testis, Pem is unique in that it is expressed exclusively in the somatic Sertoli cells (4, 5, 7). *Pem* is the founding member of the recently defined PEPP homeobox subfamily, named after the members that have so far been identified: *Pem*, *Esx-1* (*Spx-1*), *Psx-1*, and *Psx-2* (*Gpbox*) (10). All members of the PEPP family share related homeodomains interrupted by two introns at signature positions, are located on the X chromosome, and are preferentially expressed in reproductive tissues (11–15).

Pem mRNA expression in Sertoli cells first occurs when the adjacent germ cells initiate meiosis during the first wave of mouse spermatogenesis (between postpartum d 8 and 9). In adult mice testes, *Pem* mRNA and protein are expressed in a stage-specific manner in Sertoli cells; expression initiates in stages IV–VI of the seminiferous epithelial cycle, peaks at stage VII, and precipitously declines during late stage VIII (4, 5). Pem expression during these androgen-dependent stages of the seminiferous epithelial cycle (16) is consistent with our studies demonstrating that Pem's expression in Sertoli and epididymal cells depends on androgen (4, 5, 12, 17). The androgen-dependent and stage-specific expression pattern of Pem suggests that it is a good candidate to regulate secondary androgen-response genes important for stage-specific events in the testis.

Pitman *et al.* (6) (1998) created *Pem*-null mice to analyze the protein's function, but they did not uncover a functional role for Pem in these mice. Therefore, we elected to use a gain-of-function approach to examine Pem's function in the testis *in vivo*. We hypothesized that overriding the tight regulatory control of Pem expression by constitutively expressing Pem in Sertoli cells in all stages of the seminiferous epithelial cycle would enable us to discern one or more of its roles in spermatogenesis. We discovered that this dramatically increased the number of DNA-strand breaks in specific germ cell populations that normally acquire DNA strand breaks. Our ob-

Abbreviations: bGH, Bovine GH; DSB, double-strand DNA break; nt, nucleotide; RNase, ribonuclease; RPA, ribonuclease protection analysis; SSB, single-strand DNA break; tet, tetracycline; TUNEL, terminal deoxynucleotidyltransferase-mediated deoxyuridine 5′-triphosphate nick end labeling; WT, wild-type.

servations suggest that Pem regulates the expression of Sertoli-cell proteins that control DNA modification events in germ cells.

Materials and Methods

Generation of the Pem-121 transgene and transgenic mice

The mouse *Pem* gene contains four coding-region exons (exons 3–6) and two 5′-untranslated-region exons (exons 1 and 2) (4, 13). The *Pem Pp* is in the intron upstream of exon 3, and the *Pem Pd* is upstream of exon 1 (4, 18). To generate the *Pem-121* transgene that expresses Pem specifically from the *Pem Pp*, we used primers corresponding to exon 2 (5′-GTG GAC AAG AGG AAG CAC AAA-3′) and exon 6 (5′-GGG AAT CCA CCT CTT TAT TGC - 3′) to amplify mouse genomic DNA by PCR. This PCR product was then cloned into the plasmid pBluescript KS(+) at the *Eco*RV site. A *Bcl*I-*Sac*II fragment containing the bovine GH (bGH) polyadenylation site was removed from pGKneo^{5}bpA (kindly provided by Dr. Martin Matzuk, Baylor College of Medicine, Houston, TX) and inserted into the *Bam*HI-*Sac*II sites downstream of the *Pem* gene by partial digestion. A tetracycline (tet)-regulated promoter (*Ptet*) (a *Xho*I/*Sal*I fragment from pUHD13–3 (19) was introduced upstream of the *Pem* gene at the *Sal*I site to permit ectopic expression in virtually all tissues. This *Ptet* was included in the construct to permit analysis of Pem function in tissues besides the testis (to be reported elsewhere). *Ptet* is only transcribed in the presence of the tet transactivator protein; and thus, this promoter should be inactive in our tet transactivator-lacking transgenic mice. This was confirmed by ribonuclease (RNase) protection analysis (RPA), which demonstrated that *Pem* transcripts from the *Pem-121* mice were derived from the *Pem Pp* and not *Ptet* (data not shown), thus demonstrating that *Ptet* was indeed inactive. The *Pem* transcriptional unit was separated from the vector with *Xho*I and isolated as a 5.2-kb fragment on an agarose gel using Qiaex II (QIAGEN, Valencia, CA).

Transgenic mice were generated, according to standard procedures, by microinjection of gel-purified DNA (20) into fertilized F_1 (B6 × D2) eggs by the University of Texas M. D. Anderson Cancer Center Transgenic Mouse Facility. Founder *Pem-121* mice were analyzed for the presence of the *Pem-121* transgene by PCR of tail DNA with primers corresponding to the tet promoter (5′-GTT TAG TGA ACC GTC AGA TCG-3′) and exon 3 of the Pem gene (5′-TTC CGA GTC TTC CTT GAC TC-3′). The resulting PCR product was 750 bp in size. Animals were housed in standard lighting (12 h of light, 12 h of darkness) and allowed food and water *ad libitum*. They were maintained in facilities approved by the American Association for the Accreditation of Laboratory Animal Care.

Histological examination, immunohistochemistry, and terminal deoxynucleotidyltransferase-mediated deoxyuridine 5′-triphosphate nick end labeling (TUNEL) staining

Testes were collected and fixed in Bouin's solution (Sigma, St. Louis, MO) overnight, washed in a saturated solution of Li_2CO_3 in 80% ethanol to remove Bouin's fixative until dye was no longer visible in the wash solution, dehydrated, embedded in paraffin, and sectioned following standard histological procedures. Sections (10 μm) were mounted on siliconized slides and were stained for histological examination with either hematoxylin-and-eosin or periodic acid/Schiff stain. Immunohistochemical staining of testis sections was carried out as described previously (6, 21) using a polyclonal antibody specific to mouse Pem (21). For TUNEL assessment, we used the ApopTag Plus peroxidase *in situ* apoptosis detection kit (S-7101; Intergen, Purchase, NY) following the manufacturer's instructions. Sections for immunohistochemistry and TUNEL were counterstained with Harris' hematoxylin. Counts of TUNEL-positive cells in all round tubules were made on testis sections of at least three animals from each founder group.

RNA purification and analysis

Total cellular RNA from tissues was prepared by guanidinium isothiocyanate lysis and centrifugation over a cesium chloride cushion (22) and quantified by measuring optical density. [^{32}P]uridine 5′-triphosphate-labeled RNA probes were prepared for RPA by an *in vitro* transcription protocol as described previously (23). The probes were generated from sequenced cDNA fragments as follows: Probe A was generated from a DNA template prepared from the *Pem-121* transgene vector digested with *Nde*I. It contains a fragment (approximately 0.3-kb) containing 61 nucleotides (nt) of the 3′ end of exon 6 and approximately 250 nt of the bGH poly(A) region. The β-actin probe, which contains 34 nt of human β-actin exon 3, was prepared by linearizing plasmid G-98, which contains human β-actin (accession no. X00351), with *Ban*I. It was used as a positive control in annealing reactions for RPA. A century ladder template (Ambion, Inc., Austin, TX) was used to generate size markers for RNA. Probes were purified on a 6% polyacrylamide denaturing gel as described previously (9).

RPA was performed as described previously (9, 23), with minor modifications. Briefly, sample RNAs were coethanol-precipitated with the appropriate gel-purified [^{32}P]uridine 5′-triphosphate-labeled probe, and the pellet was resuspended in 10 μl annealing buffer [40 mM piperazine diethanesulfonic acid (pH 6.4), 0.4 M NaCl, 1 mM EDTA, 80% formamide] and allowed to hybridize overnight at 44 C. Unhybridized RNA was digested with RNase A (25 μg/ml) and RNase T1 (4 μg/ml) for 40 min at 30 C. The RNases were then inactivated with proteinase K treatment and extracted with phenol/chloroform/iso-amyl alcohol. After ethanol precipitation, the RNA pellet was resuspended in 90% formamide loading buffer, denatured at 85 C, electrophoresed on a 6% polyacrylamide denaturing gel, and analyzed by autoradiography and by InstantImager electronic autoradiography analysis (Packard Instruments Co., Inc., Meriden, CT).

Northern blot analysis was carried out by electrophoresis of RNA on 1% agarose denaturing (formaldehyde) gels as described previously (9), with minor modifications. Briefly, after transfer and UV cross-linking, blots were prehybridized in prehybridization buffer (50% formamide, 5-strength Denhardt's solution, 5-strength SSPE (sodium chloride-sodium phosphate-EDTA), 0.5% sodium dodecyl sulfate, and 100 μg/ml sheared fish-sperm DNA) for 30–60 min at 42 C. Blots were then hybridized with random oligomer-primed ^{32}P-labeled cloned cDNAs (prepared with a random-primer labeling kit from Roche, Indianapolis, IN) in hybridization buffer (prehybridization buffer plus 10% dextran sulfate) overnight at 42 C. The *Pem* probe consisted of full-length mouse *Pem* cDNA. Full-length cyclophilin cDNA (24) was used as a loading control.

Comet assay

Cells were prepared and lysed as previously described (25). Briefly, testes from 12- to 16-wk-old mice were removed, decapsulated, and immediately placed in ice-cold PBS. Tissues were finely chopped with a scalpel in ice-cold PBS, filtered through a 100-μm cell strainer (Falcon no. 2360), and diluted to 3×10^4 cells/ml. Aliquots of 10^4 cells were mixed with 1% (wt/vol) low-melt agarose prepared in double-distilled water and equilibrated to 42 C. The mixture was pipetted onto a frosted microscope slide and allowed to gel. For alkaline comet assay, slides were submerged in alkaline-lysis solution (0.03 M NaOH, 1 M NaCl, and 1% N-lauroyl sarcosine) for 1 h and then rinsed twice, for 30 min each, in comet buffer (0.03 M NaOH and 2 mM EDTA). All manipulations were performed in darkened conditions at room temperature. After the rinse, slides were subjected to electrophoresis at 0.6 V/cm in freshly made comet buffer for 25 min, to allow extrusion of DNA from the cells. For neutral comet assays, slides were submerged in neutral-lysis solution (0.5 M EDTA, 0.5% sodium dodecyl sulfate, pH 8.0) for 4 h at 50 C and then soaked in TBE buffer (90 mM Tris, 2 mM EDTA, 90 mM boric acid, pH 8.5) for 4 h at room temperature. Electrophoresis was performed at 0.6 V/cm in TBE for 25 min. After electrophoresis, slides for either the alkaline or neutral comet assay were rinsed for 15 min in distilled water, submerged in 2.5 μg/ml propidium iodide for 20 min, rinsed in distilled water, and placed in a humidified, air- and light-tight container until they were scored. Comets were scored using a Hamamatsu color chilled 3CCD camera (no. C5810) and a Zeiss Axioplan2 fluorescence microscope. Color TIFF images of the comets were captured using Optimas 6.5 on Windows NT and then converted to gray-scale GIF images using Photoshop 5.5 on MacOS 9.0.4. Images were then analyzed using comet analysis software (Euclid Analysis, St. Louis, MO) to determine (1) the comet tail moment (calculated using the values for comet tail length and percent of total DNA in the comet tail) and (2) total DNA content in both the cell and its tail. The former reflects the amount of broken DNA, whereas the latter reflects ploidy.

Spectrofluorimetric caspase-3 quantification

Testes from 12- to 16-wk-old mice were removed, decapsulated, and immediately placed in ice-cold PBS. Tissues were finely chopped with a scalpel in ice-cold PBS, filtered through a 100-μm cell strainer (Falcon no. 2360), and diluted to 1×10^6 cells/ml. Cells were lysed in 200 μl lysis buffer (100 mM HEPES, 10% sucrose, 0.1% 3-[(3-cholamidopropyl) dimethylammonio]-1-propanesulfonate, pH 7.5; 1 mM EDTA; 10 mM dithiothreitol; 2 mM phenylmethylsulfonylfluoride; 100 μM pepstatin; 10 μg/ml leupeptin). Lysates were incubated for 1 h on ice. Samples were divided for duplicate reactions; thus, 100 μl lysate was transferred to a fresh Eppindorf tube, and 900 μl reaction buffer (100 mM HEPES; 10% sucrose, pH 7.5; 1 mM EDTA) was added to each sample. Fluorogenic substrate specific for caspase-3 (Ac-Asp-Glu-Val-Asp-AMC ammonium salt; Bachem California, Inc., Torrance, CA) at a concentration of 25 nM (in dimethylsulfoxide) was added (4 μl) to each sample and incubated for 2 h at 37 C. Reaction buffer (1 ml) was added to each sample, and the sample was analyzed at an excitation wavelength of 380 nm and an emission wavelength of 460 nm on an RF-1501 spectrofluorimeter (Shimadzu Scientific Instruments, Columbia, MD). Relative fluorescence was calculated by subtracting the blank fluorescence (buffer plus substrate only) from the sample fluorescence value.

Results

Expression of the Pem-121 transgene in transgenic mice

To determine the function of Pem in the testis *in vivo*, we expressed it from a transgene containing *Pem's* Sertoli cell-specific promoter (the *Pem Pp*). This transgene (*Pem-121*) contained 0.6-kb of *Pem Pp* 5′-flanking sequence upstream of the *Pem* coding exons and intervening introns (Fig. 1A). Three founder animals carrying this *Pem* transgene (*Pem-121.2*, *Pem-121.5*, and *Pem-121.7*) were identified and were used to establish transgenic lines. Using a probe specific to the bGH polyadenylation region of the *Pem* transgene for RPA, we detected transgene expression in the testis of all three transgenic mice but not in wild-type (WT) control mice (Fig. 1B). Northern blot analysis with a probe specific to the *Pem* coding region demonstrated that all three transgenic mouse lines expressed higher levels of *Pem* mRNA in the testis than did littermate controls (Fig. 1C). *Pem-121.2* mice had approximately 3-fold higher *Pem* mRNA levels than did control mice, whereas *Pem-121.5* and *Pem*–121.7 mice had approximately 7-fold increased *Pem* transcript levels.

We previously demonstrated that endogenous *Pem* transcripts are expressed specifically in Sertoli cells in a stage-specific manner (primarily in stages VI–VIII) in the mouse testis (9). To determine whether the *Pem-121* transgene reproduced this cell type- and stage-specific expression, we performed immunohistochemical analysis with a rabbit

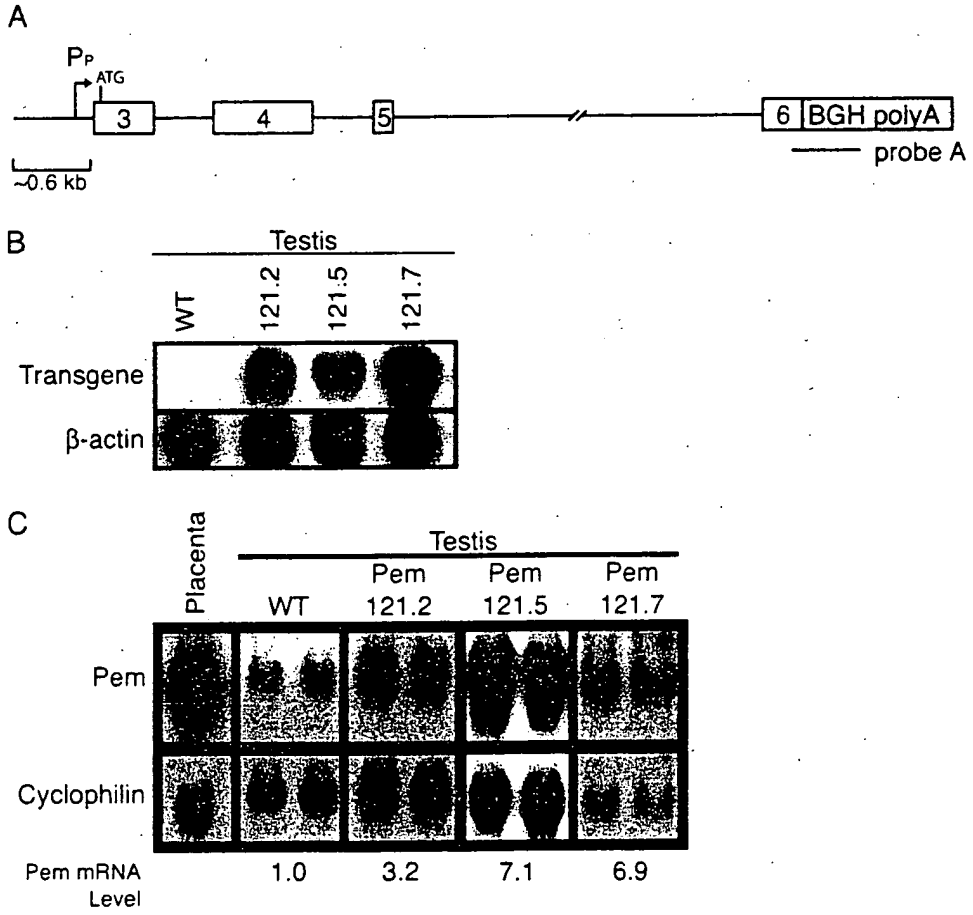

FIG. 1. A murine *Pem* transgene is expressed at high levels in the testis *in vivo*. A. Schematic diagram of the *Pem-121* transgene, showing its Sertoli cell-specific promoter (*Pem Pp*) and the bGH poly(A) region. The beginning of the coding sequence is indicated by the ATG start codon in exon 3. Probe A corresponds to the region shown. B. RPA of adult testis RNA (10 μg) from WT and three transgenic founder lines using probe A. The band size was approximately 200 nt, as judged by comparison with the migration of an RNA century ladder (data not shown). β-actin (band size, ~35 nt) was included as a loading control. C. Northern blot analysis of adult testis RNA (10 μg) from WT and three transgenic founder lines with a Pem probe that recognizes both endogenous and transgene transcripts. Placenta RNA (10 μg) from a WT mouse was used as a positive control for *Pem* expression. Cyclophilin was used as a loading and normalization control.

polyclonal antibody prepared against recombinant mouse Pem. This antibody has been previously shown to react specifically with mouse Pem, as judged by immunohistochemical analysis performed on mouse embryos and testis (4, 6, 21). Our immunohistochemical analysis demonstrated that Pem protein was at much higher levels in transgenic mouse testes than in control littermate testes (Fig. 2), consistent with the higher *Pem* mRNA levels in these mice (Fig. 1C). Pem protein was limited to Sertoli cells (primarily in their nuclei) in both transgenic and control animals; it was not observable in any germ cell population. However, in contrast with control mice, the transgenic mice expressed Pem protein in a stage-independent manner such that all Sertoli cells in all stages of the seminiferous epithelial cycle expressed Pem. This is clearly demonstrated by comparing Fig. 2, E with F; the latter shows strong Pem expression in a stage IX tubule from a *Pem-121* transgenic mouse, whereas the former shows lack of Pem expression in a stage IX tubule in a control littermate mouse. This unique expression pattern afforded us an opportunity to examine the functional consequences of *Pem-121* expression in the correct cell type but during all stages of the seminiferous epithelial cycle.

Pem expression in Sertoli cells dramatically increases the proportion of germ cells with DNA strand breaks

As part of our characterization of the effects of Pem overexpression in Sertoli cells, we used the TUNEL assay, which quantitates the free DNA ends typical of apoptosis. This analysis revealed that *Pem* transgenic mice had a dramatic increase in the number of TUNEL-positive germ cells. Two germ cell subsets displayed this response: preleptotene spermatocytes (Figs. 3, A and B, and 4A), and elongating spermatids at step 9–10 (Figs. 3, E and F, and 4C). Single-factor ANOVA and Tukey tests, the latter of which compares differences between multiple comparisons, revealed a significant difference in the percentages of both positively stained preleptotene spermatocytes [$F(3, 116) = 264.34$, $P < 0.001$] and elongating spermatids [$F(3, 56) = 27.45$, $P < 0.001$] in the three *Pem* transgenic mice lines, as compared with control littermates. The increased frequency of TUNEL-positive spermatids was specific for steps 9 and 10, as there was a normal frequency of TUNEL-positive step 11 spermatids in the *Pem* transgenic mice (data not shown). Both control and transgenic mice had apoptotic TUNEL-positive pachytene spermatocytes and round spermatids; whereas spermatogonia, leptotene spermatocytes, and elongated spermatids were not detectably TUNEL-positive (data not shown).

Despite the fact that the TUNEL assay is a standard assay for apoptosis, several lines of evidence suggest that most of the TUNEL-positive preleptotene spermatocytes and steps 9–10 elongating spermatids in *Pem-121* transgenic mice were not apoptotic. First, TUNEL staining was confined to the nuclei, whereas apoptotic germ cells typically exhibit staining throughout the entire cell. Second, we did not find other characteristics of germ cell apoptosis, such as membrane blebbing or the gross-level chromatin abnormalities. Third, we observed no overt defects in testicular morphology. Fourth, we found no dramatic depletion of germ cells, which would be expected if a large number of germ cells underwent apoptosis. For example, if the approximately 80% of preleptotene spermatocytes that are TUNEL-positive in *Pem-121* transgenic mice were truly apoptotic, we should have also observed a massive decrease in later populations of germ cells. Fifth, we found that the *Pem-121* transgenic mice did not have an increase in activated caspase-3, as measured by spectrofluorimetric caspase-3 quantification (data not shown). Sixth, the *Pem-121* transgenic mice did not have an increased frequency of TUNEL-positive pachytene spermatocytes, the cells that normally undergo apoptosis (26). We found that 6.3–16% of pachytene spermatocytes from stages XII–VI in transgenic and littermate control mice were TUNEL-positive and demonstrated the typical characteristics of apoptotic germ cells, such as disorganized chromatin and membrane blebbing (Figs. 3, C and D). Each transgenic line exhibited a different percentage of TUNEL-positive pachytene spermatocytes (Fig. 4B) that did not correlate with the levels of *Pem* mRNA expression (Fig. 1C). Statistical analysis by ANOVA and Tukey tests revealed a significant difference [$F(3, 116) = 6.80$, $P < 0.01$] in the percentages of TUNEL-positive pachytene spermatocytes in only one *Pem* transgenic mouse line (*Pem-121.2*), as compared with control littermates. We conclude that it is unlikely that Pem expression in Sertoli cells influences germ cell apoptosis.

Increased frequency of double-strand DNA breaks (DSBs) and single-strand DNA breaks (SSBs) in germ cells as a result of Pem expression in Sertoli cells

As an independent assay to assess whether ectopic Pem expression increases the frequency of DNA strand breaks, we used the alkaline comet assay. The advantage of the comet assay is that it allowed us to measure the amount of DNA strand breaks per cell and to identify and categorize cells based on DNA content. Analysis by the comet assay revealed that all three *Pem* transgenic mice lines had a significant increase in the average tail moment (the amount of DNA damage, as defined by the tail length and the percent of the total DNA in the tail) in both the haploid and tetraploid populations but not in the diploid cell population (Fig. 5, A–C). We do not believe that this increase in migrating DNA was the result of an increase in the number of apoptotic bodies, because these would have had very long tail moments, a high percentage of DNA in the tails, and a low percentage of DNA in the comet head (27). Rather, the increase in the average moment that we observed indicates a significant increase in the number of strand breaks in viable germ cells. The increase that we observed in the average tail moment in the tetraploid population is consistent with the increase in TUNEL-positive preleptotene spermatocytes in stage VIII tubules (Fig. 4A). The increase in average tail moment in the haploid population is consistent with the increase in TUNEL-positive elongating spermatids (Fig. 4C). The lack of a significant difference in average tail moments of the diploid cells between the Pem transgenic mice and control mice confirms our TUNEL assay results in which we found no increase in DNA strand breaks in diploid germ cells. Moreover, the lack of difference in tail moments in the diploid population suggests that Pem did not induce DNA strand breaks in Sertoli cells, the cells in which Pem is ex-

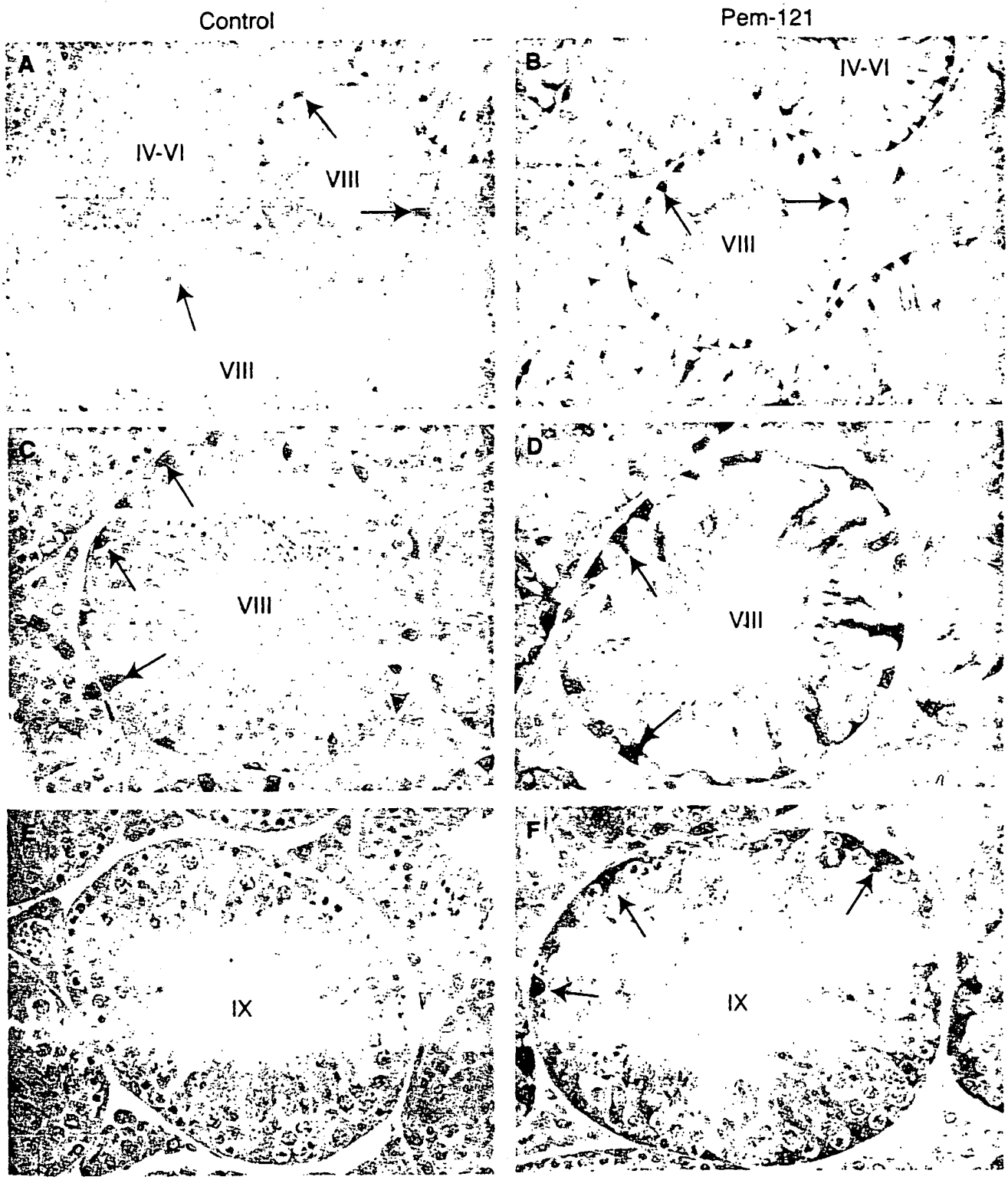

FIG. 2. Sertoli cell- and stage-specific expression of the *Pem-121* transgene *in vivo*. Immunohistochemical analysis of *Pem-121.5* (B, D, and F) adult testis sections and littermate controls (A, C, and E) using an antimouse Pem antisera. A and B, Photomicrographs of testis sections (200×) from 12-wk-old control and *Pem-121.5* mice, respectively. C–F, Photomicrographs at a higher magnification (400×). The *arrows* point to selected Sertoli cell nuclei that stain for Pem.

pressed. It should be noted that the comet assay detected a smaller difference in DNA strand breaks between the transgenic and WT mice, compared with the TUNEL assay. One explanation for this difference is that, unlike the TUNEL assay, the comet assay does not distinguish between cell types but instead distinguishes cells by ploidy. Thus, the

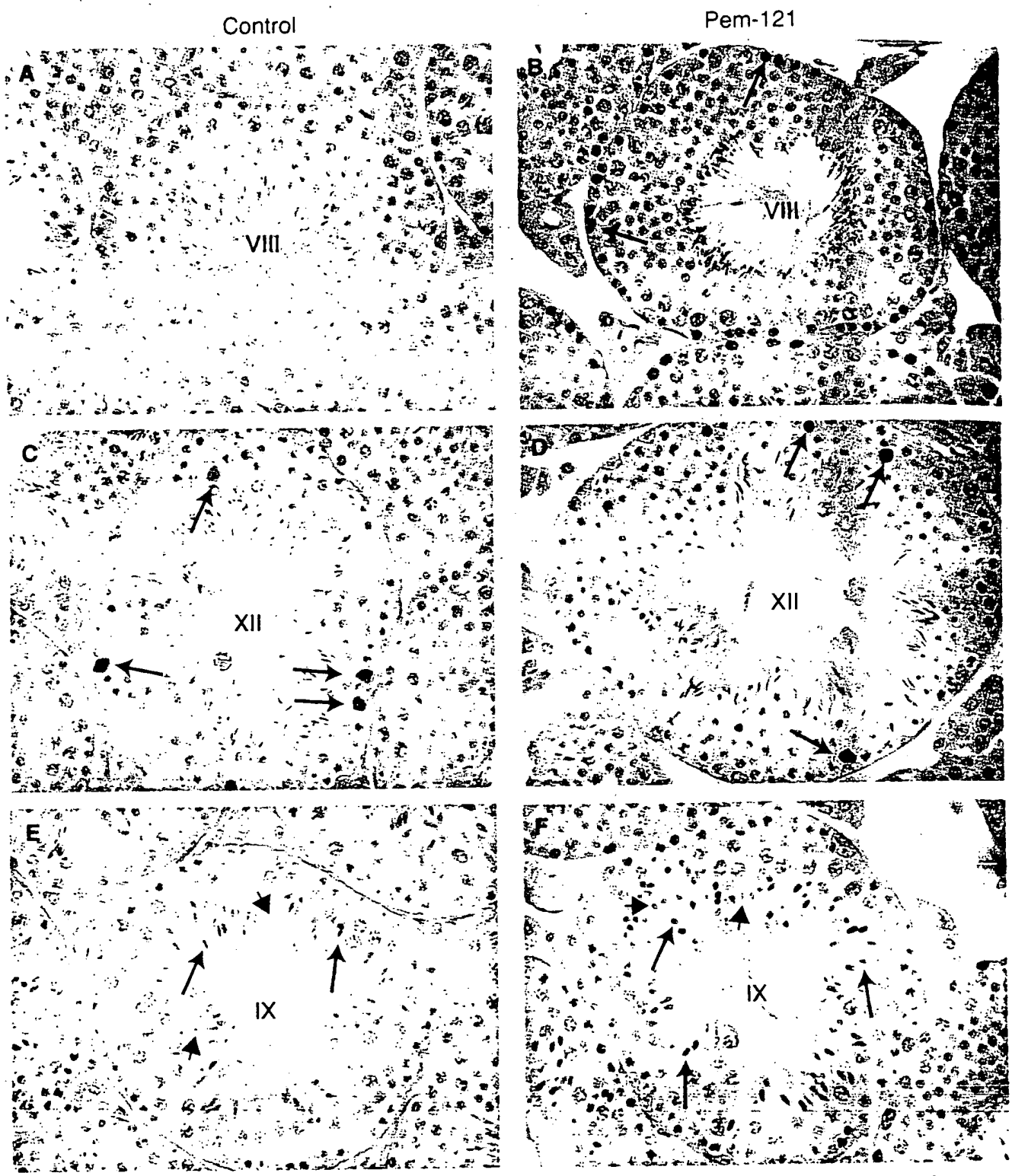

FIG. 3. *Pem* transgene expression in Sertoli cells induces the appearance of TUNEL-positive preleptotene spermatocytes and increases the frequency of TUNEL-positive elongating spermatids. Photomicrographs of testis sections (400×) from 12-wk-old control (A, C, and E) and *Pem-121.5* (B, D, and F) mice. Panel A shows a lack of TUNEL-positive preleptotene spermatocytes in control mice, whereas B shows that TUNEL-positive preleptotene spermatocytes are frequent in *Pem* transgenic mice. C and D show that both control and *Pem-121* transgenic mice have TUNEL-positive pachytene spermatocytes that have classical features of apoptosis. E shows that control mice have few TUNEL-positive step 9 elongating spermatids and that they only weakly stain by the TUNEL method. F shows that *Pem-121* transgenic mice have many TUNEL-positive step 9 elongating spermatids and that their TUNEL staining is stronger than those in control mice. The *arrows* point to selected TUNEL-positive elongating spermatids. The *short arrows* (E and F) point to TUNEL-negative elongating spermatids.

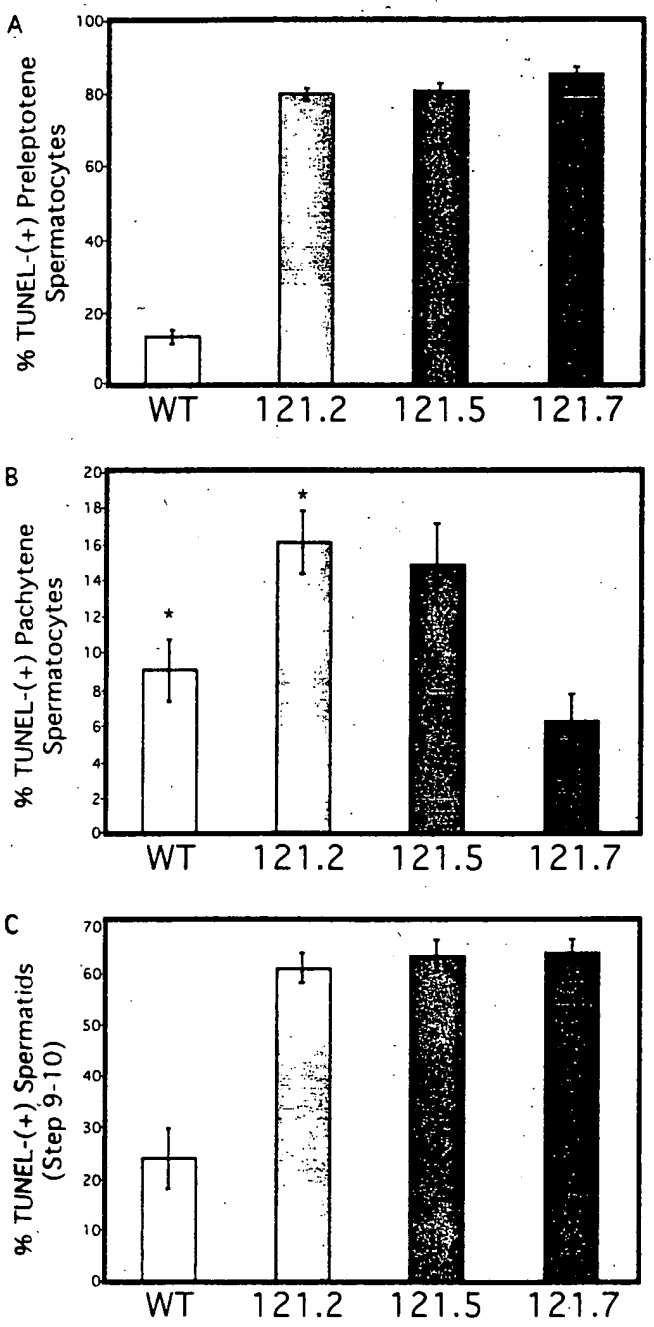

FIG. 4. Quantitative analysis of TUNEL-positive germ cell populations in the adult testis (shown as mean and SE of mean). Round tubules (n = 30 for each founder line except panel C, where n = 15) were scored. A, All three transgenic founder lines exhibit greater than a 6-fold increase in the percentage of TUNEL-positive preleptotene spermatocytes, compared with control mice ($P < 0.01$). B, Transgenic mice exhibit various amounts of TUNEL-positive pachytene spermatocytes during stages XII–VI of the seminiferous epithelial cycle. Statistical analysis demonstrated that only *Pem-121.2* was significantly different from control mice (*, $P < 0.01$). C, All three transgenic founder lines exhibit greater than a 2.5-fold increase in the percentage of TUNEL-positive steps 9 and 10 elongating spermatids, compared with control mice ($P < 0.01$). ANOVA and Tukey tests were performed to determine statistical variance. *P* values were determined using Student's *t* test (one-tailed) between those means that were determined to be significantly different by ANOVA and Tukey tests.

comet assay would measure DNA breaks in all haploid cells, not just elongating spermatids, which would dampen effects observed.

To ascertain the nature of the DNA strand breaks, we elected to use the neutral comet assay, which does not denature DNA; and so, only DNA with DSBs are able to migrate from the head and form the tail of the comet. Thus, comet moments observed under neutral conditions indicate the presence of DSBs and not SSBs. We observed a significant increase in the average comet moment in the tetraploid population for all three transgenic lines, compared with controls [$F(3, 77) = 5.55$, $P < 0.01$] (Fig. 5D). In contrast, we found no significant difference in either the haploid [$F(3, 224) = 2.19$, $P < 0.09$] or diploid [$F(3, 85) = 1.54$, $P < 0.25$] populations for all three transgenic lines, compared with control mice (Fig. 5D). These observations, coupled with our alkaline comet results, suggest that the increase in DNA strand breaks that we observed in elongating spermatids were SSBs, whereas the breaks we observed in preleptotene spermatocytes were DSBs. Although our analysis does not rule out the possibility that preleptotene spermatocytes also had some SSBs (because the alkaline comet assay does not distinguish between SSBs and DSBs), the combined results from the neutral and alkaline comet assays strongly support our contention that Pem overexpression in Sertoli cells results in an increase in specific types of DNA strand breaks in distinct germ cell populations.

Effect of Pem overexpression in Sertoli cells on fertility and germ cell subsets

Despite the dramatically increased frequency of preleptotene spermatocytes and elongating spermatids possessing increased DNA strand breaks in *Pem* transgenic mice, these mice had no obvious disruption of spermatogenesis or any overt histological anomalies in the seminiferous tubules, as judged by histological examination of hematoxylin-and-eosin- and periodic acid/Schiff-stained sections (data not shown). *Pem* transgenic mice also exhibited normal fertility, given that there was no significant difference in litter sizes born to WT (6.40 ± 0.29) and transgenic parents (*Pem-121.2*, 6.34 ± 0.31; *Pem-121.5*, 6.92 ± 0.22; and *Pem-121.7*, 7.03 ± 0.22).

However, we obtained evidence that the *Pem* transgenic mice had modest alterations in specific germ cell subsets. Statistical analysis, using ANOVA, revealed that there was a statistically significant increase in the mean number of steps 9–10 elongating spermatids per tubule in the three transgenic lines, as compared with the control mice [$F(3, 56) = 4.97$, $P < 0.005$] (Fig. 6C). The Tukey test demonstrated that the three *Pem* transgenic lines did not have statistically significant differences between them, indicating that the effect was attributable to Pem (Fig. 6C). The mean number of preleptotene spermatocytes per tubule was also slightly greater in all three transgenic lines, compared with control littermates (Fig. 6A). However, ANOVA and Tukey analysis demonstrated that only one transgenic line, *Pem-121.7*, exhibited a significant difference, compared with control littermates [$F(3, 116) = 7.78$, $P < 0.001$]. Statistical analysis of pachytene spermatocytes in stages XII–VI of the seminiferous epithelial cycle

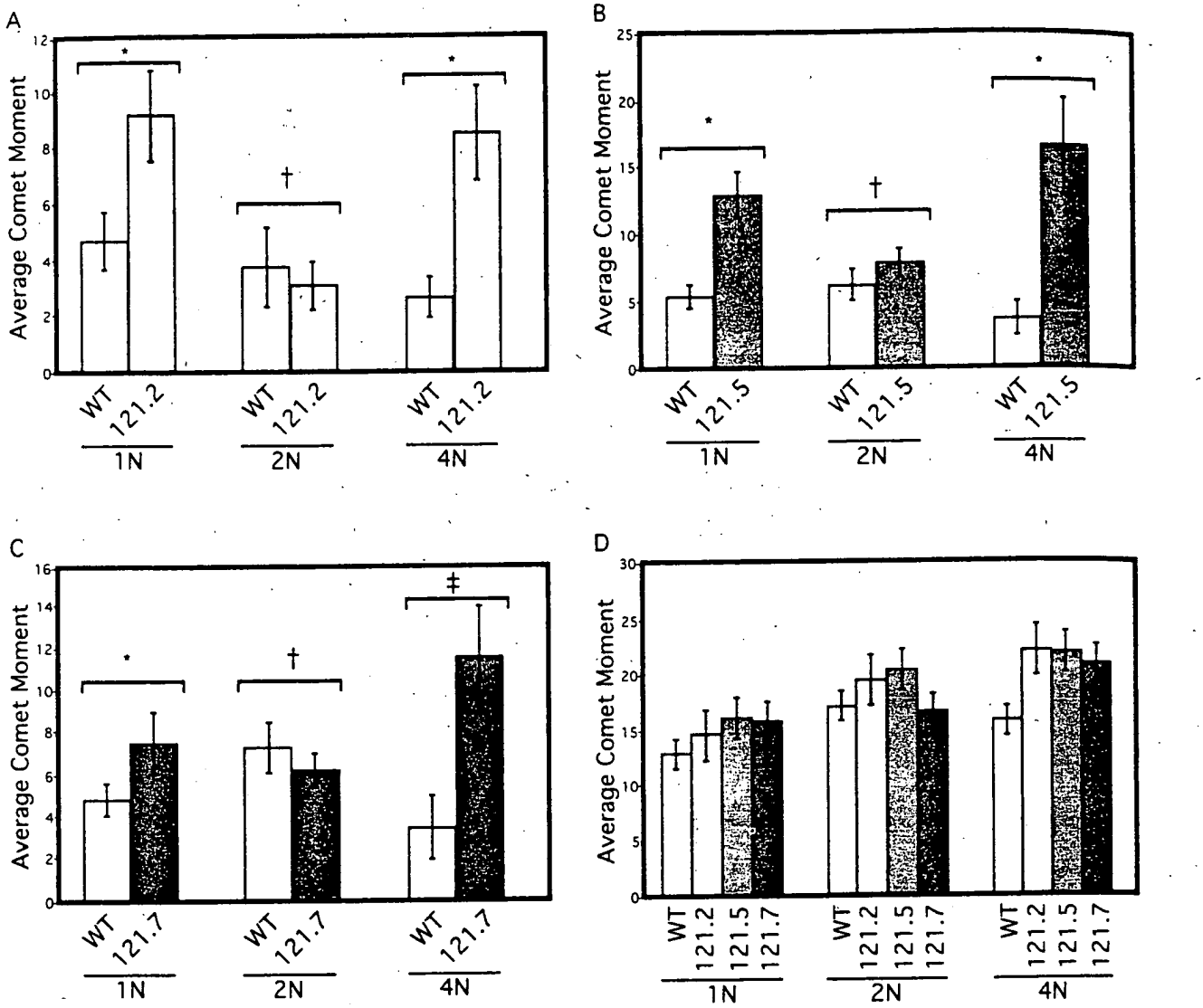

FIG. 5. *Pem* transgenic mice exhibit more DNA strand breaks, as assessed by comet assay. A–C demonstrate an increase in average comet moments in all three transgenic mice lines in both the haploid and tetraploid, but not in the diploid populations, as assessed by the alkaline comet method. A, *Pem-121.2* compared with littermate control; *, $P < 0.01$ for 1N and 4N; †, $P < 0.35$ for 2N. B, *Pem-121.5* compared with littermate control; *, $P < 0.01$ for 1N and 4N; †, $P < 0.15$ for 2N. C, *Pem-121.7* compared with littermate control; *, $P < 0.05$ for 1N; †, $P < 0.25$ for 2N; ‡, $P < 0.02$ for 4N. D, Increase in average tail moments for all three transgenic lines in the tetraploid population, but not in the haploid or diploid population, as assessed by the neutral comet assay. Statistical analysis was performed as described for Fig. 4.

demonstrated a statistically significant difference between two of the transgenic lines, compared with control littermates [$F(3, 116) = 21.13$, $P < 0.001$] (Fig. 6B). However, these two transgenic lines displayed a different response (*Pem-121.2* showed an increase and *Pem-121.7* showed a decrease), indicating that the changes in pachytene spermatocytes were unlikely to be attributable to Pem overexpression.

Discussion

In this communication, we report that Pem expression in Sertoli cells increases the number of germ cells with DNA strand breaks. We demonstrated this in transgenic mouse lines that specifically express Pem in Sertoli cells during all stages of the seminiferous epithelial cycle, rather than in a stage-specific manner (IV–VIII), as Pem is normally. The effect of Pem's aberrant expression on DNA strand breaks was observable only in the adjacent germ cells that were present during and immediately after the stages where Pem is normally expressed. In particular, we found an increased frequency of preleptotene spermatocytes with DSBs (stages VII–VIII) and steps 9–10 elongating spermatids with SSBs (stages IX–X). This conclusion was supported by three lines of evidence: 1) the number of cells in these germ cell subsets that were TUNEL-positive was dramatically increased in *Pem* transgenic mice (Fig. 4, A and C); 2) haploid and tetraploid germ cells in transgenic *Pem* mice demonstrated an increase in average tail length and percentage of DNA in the tail when assayed by the alkaline-comet assay (Fig. 5, A–C); and 3) there was a significant increase in free-DNA ends in tetraploid germ cells in *Pem* transgenic mice, as assayed by

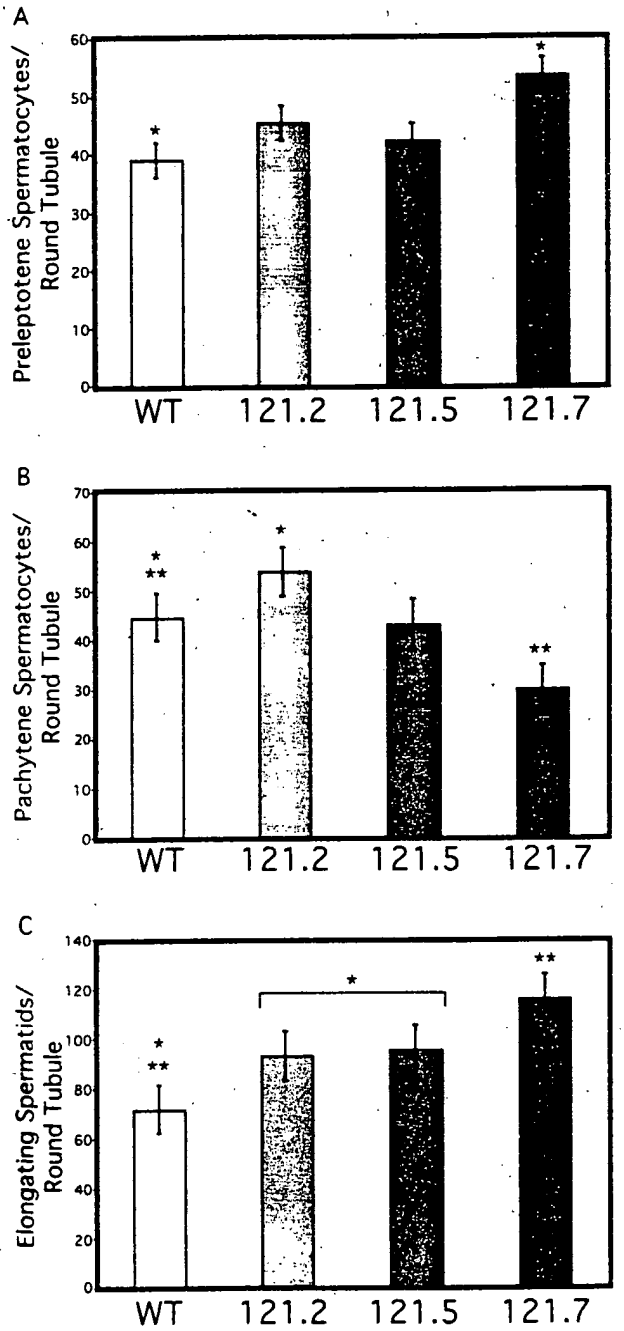

FIG. 6. Quantitative analysis of germ cell populations in the adult testis (shown as mean and SE of mean). Round tubules (n = 30 for each founder line except C, where n = 15) were scored for the number of germ cells present. A, Preleptotene spermatocytes during stage VIII of the seminiferous epithelial cycle. *, $P < 0.001$ for comparison between *Pem-121.7* and WT. B, Pachytene spermatocytes during stage XII–VI. *, $P < 0.002$ for comparison between *Pem-121.2* and WT. **, $P < 0.001$ for comparison between *Pem-121.7* and WT. C, Step 9–10 elongating spermatids from stage IX and X. *, $P < 0.02$ for comparison of *Pem-121.2* and *Pem-121.5* to WT. **, $P < 0.001$ for comparison of *Pem-121.7* and WT. Statistical analysis was performed as described for Fig. 4.

the neutral-comet assay (Fig. 5D). Though this data implicates Pem as a potent regulator of germ cell events, it should be stressed that our results were obtained from transgenic mice that ectopically express Pem; and thus, we cannot be sure that Pem's normal physiological role is to control DNA strand breaks in germ cells.

Many other transcription factors are expressed in Sertoli cells, including GATA-1, GATA-4, WT-1, Sox9, SF-1, and Spz-1 (28–32), but Pem is the first to be suggested to play a role in the adult testis. Our observations suggest a model in which Pem regulates Sertoli-cell genes that encode secreted or cell-surface proteins that signal germ cells to alter DNA replication, DNA repair, or chromatin remodeling. The discovery that Pem expression in Sertoli cells alters the number of preleptotene spermatocytes and spermatids with DNA modifications is significant, because little is known about how Sertoli cells influence germ cell maturation events (1, 3).

Although there are many differences between preleptotene spermatocytes and elongating spermatids, two features they share in common are their high degree of chromatin remodeling and their positions at critical points of germ cell differentiation. Preleptotene spermatocytes are at the important juncture in which mitosis has ceased and meiosis has begun. During this stage, their chromatin undergoes reorganization as meiotic replication begins. Steps 9–10 haploid spermatids are also at a critical point of differentiation because they are undergoing cellular elongation and repackaging of their chromatin into a more condensed state. At step 10 in the mouse, histones become acetylated and begin to disassociate from DNA as they are replaced by the transition proteins (33).

Spermatocytes normally begin to accumulate DSBs during premeiotic S-phase (34). Why does Pem expression in Sertoli cells increase the proportion of preleptotene spermatocytes with these DSBs? One possible explanation is that Pem affects meiotic DNA replication by increasing topoisomerase activity, which would result in increased DNA nicking (SSBs) and a subsequent increase in DSBs caused by replication-fork stalling (35, 36). To date, the presence of topoisomerases in preleptotene spermatocytes has not been investigated. However, topoisomerase IIα has been found to be present in meiotic prophase spermatocytes (37), and recent work in the rat has demonstrated that its expression is androgen-dependent (38), just as Pem is (5, 17). Furthermore, topoisomerase IIα has been localized to sites of DNA replication in chicken embryonic fibroblasts, suggesting that it plays a role in DNA unwinding during replication (39). Interestingly, in the mouse testis, topoisomerase IIα expression is initiated at d 8 (37), the same time that Pem expression is initiated (5). An alternative explanation is that Pem may promote a delay in the repair of DSBs by inhibiting either the production or activity of DNA-repair molecules. Targets for such regulation are the several ligases that repair DSBs resulting from DNA replication and recombination (40–42). Other potential targets are the many molecules localized at DSBs and arrested replication forks that collaborate to direct cell-cycle checkpoints that act during premeiotic S-phase, including H2AX-γ, ATM, BRCA1, PCNA, Mre11, Rad50, and 53BP1 (34, 43–47). Regardless of the exact mechanism, the lack of detectable strand breaks in leptotene spermatocytes from *Pem-121* transgenic mice suggests that the breaks we observed in preleptotene spermatocytes are repaired and do not hinder gametogenesis.

During steps 9–10 of spermiogenesis, spermatids repackage and remodel their chromatin into a more condensed state (33), which results in the formation of transient SSBs, probably as a result of the mechanical manipulation of the DNA to eliminate the presence of supercoiled DNA (48–50). The increase in the number of spermatids with SSBs caused by Pem expression in Sertoli cells suggests that this chromatin remodeling process may be directed by a Pem-induced Sertoli-cell signal. Though no proteins have yet been identified as responsible for causing these SSBs in spermatids, topoisomerase II is a likely candidate, because it has been localized to the chromosomes in nuclei of elongating spermatids in the rat (33). This enzyme is believed to serve as a loop fastener that organizes chromatin into loop domains, based on studies that show that topoisomerase II binds to chromosomal scaffolds in the nuclear matrices of somatic cells (33, 51, 52). Alternatively, Pem may not actually increase the frequency of SSB induction; but rather, it may increase the persistence of SSBs at a given point in time by delaying or inhibiting DNA repair. Regardless, it is clear that SSBs are necessary to relieve the torsional stress in DNA to better suit the conditions needed for the major structural rearrangement of chromatin in germ cells in later spermiogenesis (33), and our data suggests the possibility that Pem directs this activity via the Sertoli cell. It is likely that these strand breaks are repaired between steps 10 and 11, because we were unable to detect DNA strand breaks in step 11 spermatids. Because SSBs in spermatids are repaired as part of the normal program of spermiogenesis (33, 48), this underscores the likelihood that Pem impinges on a normal developmental pathway rather than directing an aberrant process. This is further supported by our finding that our *Pem-121* transgenic mice were fertile and had no gross level alterations in seminiferous epithelial morphology.

The increase in DNA strand breaks caused by Pem expression in Sertoli cells was limited to germ cells in stages VII–X, despite the presence of Pem, in all stages of the seminiferous epithelial cycle in our transgenic mice (Figs. 2 and 3). This selectivity correlates with Pem's normal expression pattern in the mouse: Pem is dramatically induced in Sertoli cells when the adjacent germ cells are at the preleptotene stage (at d 8 post partum during the first wave of spermatogenesis), and its expression is extinguished just before elongating spermatids reach step 9 (in the adult seminiferous epithelial cycle) (4, 5). It will be interesting to determine whether this selectivity occurs at the level of the Sertoli cell or the germ cell. If at the level of the Sertoli cell, it may be attributable to a stage-specific inhibitor of Pem function or stage-specific alterations in Pem's downstream genes that make them impervious to Pem regulation at stages other than VII–X. If at the level of the germ cell, perhaps only specific germ cell subsets are competent to receive a Pem-induced Sertoli-cell signal. The differentiation program of germ cells may dictate this receptivity. For example, the initiation of meiotic replication may induce receptivity to the Pem-induced signal, thus explaining why preleptotene spermatocytes respond but not mitotic spermatogonia. In yeast, meiotic DNA replication is distinguished from mitotic replication by promitotic cyclins and the promeiotic molecule Ime I (53); such molecules could also dictate receptivity to Pem-induced signals in mammalian germ cells. It is less clear what molecules might suppress receptivity in meiotic spermatocytes in prophase I, reinitiate receptivity in step 9 spermatids, and again suppress it at a later stage of spermatid differentiation.

Our findings suggest that the role of the Sertoli cell extends beyond the support role of providing nutrients to germ cells. In the future, it will be important to identify the Pem-induced molecules secreted or expressed on the surface of Sertoli cells that mediate this communication between Sertoli cells and germ cells. That Pem functions in activating signaling between somatic and germ cells is consistent with the fact that in the ovary, Pem is expressed by granulosa cells, the somatic cells that surround the oocyte (6). Pem is also aberrantly expressed in tumor cells from several different lineages and tissues (18); and thus, it is possible that it also plays a role in tumor-cell progression by allowing tumor cells to circumvent normal checkpoint mechanisms that survey DNA strand breaks and control cell-cycle progression (54).

Acknowledgments

We would like to thank David McConkey for his assistance in our apoptosis studies.

Received May 28, 2002. Accepted August 22, 2002.

Address all correspondence and requests for reprints to: Miles F. Wilkinson, Department of Immunology, Box 180, University of Texas M. D. Anderson Cancer Center, 1515 Holcombe Boulevard, Houston, Texas 77030. E-mail: mwilkins@mail.mdanderson.org.

This work was supported by NIH Grant CA-78023.

References

1. **Russell LD, Griswold MD** 1993 The Sertoli cell. 1st ed. Clearwater, FL: Cache River Press
2. **Fujisawa M** 2001 Cell-to-cell cross-talk in the testis. Urol Res 29:144–151
3. **Griswold MD** 1995 Interactions between germ cells and Sertoli cells in the testis. Biol Reprod 52:211–216
4. **Sutton KA, Maiti S, Tribley WA, Lindsey JS, Meistrich ML, Bucana CD, Sanborn BM, Joseph DR, Griswold MD, Cornwall GA, Wilkinson MF** [illegible] Androgen regulation of the Pem homeodomain gene in mice and rat Sertoli and epididymal cells. J Androl 19:21–30
5. **Lindsey JS, Wilkinson MF** 1996 Pem: a testosterone- and LH-regulated homeobox gene expressed in mouse Sertoli cells and epididymis. Dev Biol 177:471–484
6. **Pitman JL, Lin TP, Kleeman JE, Erickson GF, MacLeod CL** 1998 Normal reproductive and macrophage function in Pem homeobox gene-deficient mice. Dev Biol 202:196–214
7. **Maiti S, Meistrich ML, Wilson G, Shetty G, Marcelli M, McPhaul MJ, Morris PL, Wilkinson MF** 2001 Irradiation selectively inhibits expression from the androgen-dependent Pem homeobox gene promoter in Sertoli cells. Endocrinology 142:1567–1577
8. **Duboule D** 1994 Guidebook to the homeobox genes. Oxford: Oxford University Press
9. **Lindsey S, Wilkinson MF** 1996 Homeobox genes and male reproductive development. J Assist Reprod Genet 13:182–192
10. **Rao M, Wilkinson MF** 2002 Homeobox genes and the male reproductive tract. In: Robaire B, Hinton BT, eds. The epididymis: from molecules to clinical practice. New York: Kluwer Academic/Plenum Publishers; 269–283
11. **Sutton KA, Wilkinson MF** 1997 The rapidly evolving Pem homeobox gene and Agtr2, Ant2, and Lamp2 are closely linked in the proximal region of the mouse X chromosome. Genomics 45:447–450
12. **Maiti S, Doskow J, Li S, Nhim RP, Lindsey JS, Wilkinson MF** 1996 The Pem homeobox gene. Androgen-dependent and -independent promoters and tissue-specific alternative RNA splicing. J Biol Chem 271:17536–17546
13. **Maiti S, Doskow J, Sutton K, Nhim RP, Lawlor DA, Levan K, Lindsey JS, Wilkinson MF** 1996 The Pem homeobox gene: rapid evolution of the homeodomain, X chromosomal localization, and expression in reproductive tissue. Genomics 34:304–316
14. **Li Y, Lemaire P, Behringer RR** 1997 Esx1, a novel X chromosome-linked homeobox gene expressed in mouse extraembryonic tissues and male germ cells. Dev Biol 188:85–95

15. **Han YJ, Lee YH, Chun JY** 2000 Identification and characterization of Psx-2, a novel member of the Psx (placenta-specific homeobox) family. Gene 241: 149–155
16. **Shan LX, Zhu LJ, Bardin CW, Hardy MP** 1995 Quantitative analysis of androgen receptor messenger ribonucleic acid in developing Leydig cells and Sertoli cells by *in situ* hybridization. Endocrinology 136:3856–3862
17. **Lindsey JS, Wilkinson MF** 1996 An androgen-regulated homeobox gene expressed in rat testis and epididymis. Biol Reprod 55:975–983
18. **Wilkinson MF, Kleeman J, Richards J, MacLeod CL** 1990 A novel oncofetal gene is expressed in a stage-specific manner in murine embryonic development. Dev Biol 141:451–455
19. **Gossen M, Bujard H** 1992 Tight control of gene expression in mammalian cells by tetracycline-responsive promoters. Proc Natl Acad Sci USA 89:5547–5551
20. **Hogan B, Costantini F, Lacy E** 1986 Manipulating the mouse embryo: a laboratory manual. Cold Spring Harbor, NY: Cold Spring Harbor Laboratory
21. **Lin TP, Labosky PA, Grabel LB, Kozak CA, Pitman JL, Kleeman J, MacLeod CL** 1994 The Pem homeobox gene is X-linked, and exclusively expressed in extraembryonic tissues during early murine development. Dev Biol 166: 170–179
22. **Wilkinson M** 2000 Purification of RNA. In: Brown TA, ed. Essential molecular biology. 2nd ed. New York: Oxford University Press; 69–88
23. **Ausubel FM** 1987 Current protocols in molecular biology. Brooklyn, NY: Greene Publishing Associates
24. **Carter MS, Li S, Wilkinson MF** 1996 A splicing-dependent regulatory mechanism that detects translation signals. EMBO J 15:5965–5975
25. **Zheng H, Olive PL** 1997 Influence of oxygen on radiation-induced DNA damage in testicular cells of C3H mice. Int J Radiat Biol 71:275–282
26. **Blanco-Rodriguez J, Martinez-Garcia C** 1996 Spontaneous germ cell death in the testis of the adult rat takes the form of apoptosis: re-evaluation of cell types that exhibit the ability to die during spermatogenesis. Cell Prolif 29:13–31
27. **Olive PL, Banath JP, Durand RE** 1990 Detection of etoposide resistance by measuring DNA damage in individual Chinese hamster cells. J Natl Cancer Inst 82:779–783
28. **Ito E, Toki T, Ishihara H, Ohtani H, Gu L, Yokoyama M, Engel JD, Yamamoto M** 1993 Erythroid transcription factor GATA-1 is abundantly transcribed in mouse testis. Nature 362:466–468
29. **Ketola I, Rahman N, Toppari J, Bielinska M, Porter-Tinge SB, Tapanainen JS, Huhtaniemi IT, Wilson DB, Heikinheimo M** 1999 Expression and regulation of transcription factors GATA-4 and GATA-6 in developing mouse testis. Endocrinology 140:1470–1480
30. **Hsu SH, Shyu HW, Hsieh-Li HM, Li H** 2001 Spz1, a novel bHLH-Zip protein, is specifically expressed in testis. Mech Dev 100:177–187
31. **Lala DS, Rice DA, Parker KL** 1992 Steroidogenic factor 1, a key regulator of steroidogenic enzyme expression, is the mouse homolog of fushi tarazu-factor I. Mol Endocrinol 6:1249–1258
32. **Morais da Silva S, Hacker A, Harley V, Goodfellow P, Swain A, Lovell-Badge R** 1996 Sox9 expression during gonadal development implies a conserved role for the gene in testis differentiation in mammals and birds. Nat Genet 14:62–68
33. **McPherson S, Longo FJ** 1993 Chromatin structure-function alterations during mammalian spermatogenesis: DNA nicking and repair in elongating spermatids. Eur J Histochem 37:109–128
34. **Mahadevaiah SK, Turner JM, Baudat F, Rogakou EP, de Boer P, Blanco-Rodriguez J, Jasin M, Keeney S, Bonner WM, Burgoyne PS** 2001 Recombinational DNA double-strand breaks in mice precede synapsis. Nat Genet 27:271–276
35. **Cox MM, Goodman MF, Kreuzer KN, Sherratt DJ, Sandler SJ, Marians KJ** 2000 The importance of repairing stalled replication forks. Nature 404:37–41
36. **Kuzminov A** 2001 Single-strand interruptions in replicating chromosomes cause double-strand breaks. Proc Natl Acad Sci USA 98:8241–8246
37. **Cobb J, Reddy RK, Park C, Handel MA** 1997 Analysis of expression and function of topoisomerase I and II during meiosis in male mice. Mol Reprod Dev 46:489–498
38. **Bakshi RP, Galande S, Bali P, Dighe R, Muniyappa K** 2001 Developmental and hormonal regulation of type II DNA topoisomerase in rat testis. J Mol Endocrinol 26:193–206
39. **Niimi A, Suka N, Harata M, Kikuchi A, Mizuno S** 2001 Co-localization of chicken DNA topoisomerase IIα, but not β, with sites of DNA replication and possible involvement of a C-terminal region of α through its binding to PCNA. Chromosoma 110:102–114
40. **Higashitani A, Tabata S, Endo H, Hotta Y** 1990 Purification of DNA ligases from mouse testis and their behavior during meiosis. Cell Struct Funct 15:67–72
41. **Chen J, Tomkinson AE, Ramos W, Mackey ZB, Danehower S, Walter CA, Schultz RA, Besterman JM, Husain I** 1995 Mammalian DNA ligase III: molecular cloning, chromosomal localization, and expression in spermatocytes undergoing meiotic recombination. Mol Cell Biol 15:5412–5422
42. **Schar P, Herrmann G, Daly G, Lindahl T** 1997 A newly identified DNA ligase of Saccharomyces cerevisiae involved in RAD52-independent repair of DNA double-strand breaks. Genes Dev 11:1912–1924
43. **Ohta K, Nicolas A, Furuse M, Nabetani A, Ogawa H, Shibata T** 1998 Mutations in the MRE11, RAD50, XRS2, and MRE2 genes alter chromatin configuration at meiotic DNA double-stranded break sites in premeiotic and meiotic cells. Proc Natl Acad Sci USA 95:646–651
44. **Merino ST, Cummings WJ, Acharya SN, Zolan ME** 2000 Replication-dependent early meiotic requirement for Spo11 and Rad50. Proc Natl Acad Sci USA 97:10477–10482
45. **Ward IM, Chen J** 2001 Histone H2AX is phosphorylated in an ATR-dependent manner in response to replicational stress. J Biol Chem 276:47759–47762
46. **Rappold I, Iwabuchi K, Date T, Chen J** 2001 Tumor suppressor p53 binding protein 1 (53BP1) is involved in DNA damage-signaling pathways. J Cell Biol 153:613–620
47. **Andegeko Y, Moyal L, Mittelman L, Tsarfaty I, Shiloh Y, Rotman G** 2001 Nuclear retention of ATM at sites of DNA double strand breaks. J Biol Chem 276:38224–38230
48. **Caron N, Veilleux S, Boissonneault G** 2001 Stimulation of DNA repair by the spermatidal TP1 protein. Mol Reprod Dev 58:437–443
49. **Sakkas D, Urner F, Bizzaro D, Manicardi G, Bianchi PG, Shoukir Y, Campana A** 1998 Sperm nuclear DNA damage and altered chromatin structure: effect on fertilization and embryo development. Hum Reprod 13(Suppl 4): 11–19
50. **Smith A, Haaf T** 1998 DNA nicks and increased sensitivity of DNA to fluorescence in situ end labeling during functional spermiogenesis. Biotechniques 25:496–502
51. **Roca J, Mezquita C** 1989 DNA topoisomerase II activity in nonreplicating, transcriptionally inactive, chicken late spermatids. EMBO J 8:1855–1860
52. **McPherson SM, Longo FJ** 1993 Nicking of rat spermatid and spermatozoa DNA: possible involvement of DNA topoisomerase II. Dev Biol 158:122–130
53. **Lee B, Amon A** 2001 Meiosis: how to create a specialized cell cycle. Curr Opin Cell Biol 13:770–777
54. **Khanna KK, Jackson SP** 2001 DNA double-strand breaks: signaling, repair and the cancer connection. Nat Genet 27:247–254